Relevant energy ranges for astrophysical reaction rates

Thomas Rauscher*
Department of Physics, University of Basel, Klingelbergstr. 82, CH-4056 Basel, Switzerland
(Received 11 February 2010; published 29 April 2010)

Effective energy windows (Gamow windows) of astrophysical reaction rates for (p,γ), (p,n), (p,α), (α,γ), (α,n), (α,p), (n,γ), (n,p), and (n,α) on targets with $10 \leqslant Z \leqslant 83$ from proton to neutron dripline are calculated using theoretical cross sections. It is shown that widely used approximation formulas for the relevant energy ranges are not valid for a large number of reactions relevant to hydrostatic and explosive nucleosynthesis. The influence of the energy dependence of the averaged widths on the location of the Gamow windows is discussed and the results are presented in tabular form.

DOI: 10.1103/PhysRevC.81.045807 PACS number(s): 98.80.Ft, 26.50.+x, 26.90.+n, 24.60.Dr

I. INTRODUCTION

Astrophysical reaction rates describe the change in abundances of nuclei owing to nuclear processes in an astrophysical environment, such as a hot plasma composed of free electrons and atomic nuclei. The reaction rate per particle pair (or reactivity) is found by folding interaction cross sections σ with the appropriate energy distribution of the interacting particles in the plasma. For nucleons and nuclei interacting with each other in stars, the latter is the Maxwell-Boltzmann (MB) distribution, leading to the definition of the reactivity $\mathcal{R} = F\mathcal{I}$ with [1,2]

$$F = \sqrt{\frac{8}{\pi\mu}}\left(\frac{1}{kT}\right)^{\frac{3}{2}}, \tag{1}$$

$$\mathcal{I} = \int_0^\infty \sigma(E) E e^{-E/(kT)}\, dE, \tag{2}$$

where k denotes the Boltzmann constant, T the plasma temperature, and μ the reduced mass $\mu = M_1 M_2/(M_1 + M_2)$. Although the integration limits run from zero to infinity, the largest contributions to the integral $\mathcal{I}$ stem from a narrowly confined energy range, depending on the energy dependence of the cross sections and the MB distribution. This relevant energy range has been termed the Gamow window for charged-particle reactions and is important for both nuclear experimentalists and theoreticians, as it defines the energy window within which the reaction cross sections have to be known.

Owing to their importance, simple approximation formulas [see Eqs. (8), (9), (13), and (14)] have been derived to estimate the effective energy windows for reactions (see next sections) and are frequently used. However, the derivations of these formulas make implicit assumptions that are not always valid and therefore they cannot be applied to a number of important cases. For example, it has been pointed out [1,3] that resonances below the conventionally computed Gamow window may contribute significantly to the reaction rate for narrow-resonance capture of charged particles on light targets. It is shown in the following that this can be understood by a more appropriate treatment of the Gamow window calculation. The applicability of the approximation is discussed in more detail and the appropriate energy windows are derived quantitatively for charged-particle-induced reactions (Sec. II) and for neutral projectiles (Sec III). Section IV concludes with a discussion of the validity of the present approach and a brief summary.

II. CHARGED-PARTICLE REACTIONS

A. The standard approximation of the Gamow window

The standard approximation of the Gamow window assumes that the energy dependence of the cross section σ is mainly determined by the projectile's penetration of the Coulomb barrier. The integral $\mathcal{I}$ can then be rewritten as [1,2]

$$\mathcal{I} = \int_0^\infty S(E) e^{-E/(kT)} e^{-2\pi\eta}\, dE, \tag{3}$$

where S is the astrophysical S factor,

$$S = \sigma E e^{2\pi\eta}, \tag{4}$$

which is assumed to be only weakly dependent on the energy E for nonresonant reactions. The second exponential in Eq. (3) contains an approximation of the Coulomb penetration through the Sommerfeld parameter,

$$\eta = \frac{Z_1 Z_2 e^2}{\hbar}\sqrt{\frac{\mu}{2E}}, \tag{5}$$

where Z_1 and Z_2 are the charges of the projectile and target, respectively, and μ is the reduced mass. While the first exponential decreases with increasing energy, this second one increases, leading to a confined peak of the integrand, the so-called Gamow peak. The location of the peak E_0 is shifted to higher energies with respect to the maximum of the MB distribution at $E_{\mathrm{MB}} = kT$. Assuming a constant S factor, E_0 can be determined analytically to be [1,2]

$$E_0 = \left(\frac{\mu}{2}\right)^{\frac{1}{3}} (kT)^{\frac{2}{3}}. \tag{6}$$

*thomas.rauscher@unibas.ch

The peak is not symmetrical around E_0 but, nevertheless, is often approximated by a Gaussian function,

$$\mathcal{I}(E) = \mathcal{I}_{\max} e^{-[4(E-E_0)^2]/\Delta^2}, \tag{7}$$

where $\mathcal{I}_{\max} = \exp[-3E_0/(kT)]$ is the maximal value of the product of the two exponentials in Eq. (3) and $\Delta = 4\sqrt{E_0 kT/3}$ is the $1/e$ width of the peak. Inserting the proper numerical factors and units in Eqs. (6) and (7) leads to the more practical form [1,2,4]

$$E_0 = 0.12204\left(\mu_A Z_1^2 Z_2^2 T_9^2\right)^{\frac{1}{3}}, \tag{8}$$

$$\Delta = 0.23682\left(\mu_A Z_1^2 Z_2^2 T_9^5\right)^{\frac{1}{6}}. \tag{9}$$

Here E_0 and Δ are in units of mega–electron volts, T_9 is the plasma temperature in gigakelvins, and $\mu_A = A_1 A_2/(A_1 + A_2)$ is the reduced mass number. Equations (8) and (9) are widely used to determine a relevant energy range $E_0 - (\Delta/2) \leqslant E \leqslant E_0 + (\Delta/2)$ within which the nuclear cross sections have to be known. This is especially important and is often used to design experiments.

B. Criticism of the standard approximation

The derivation of Eq. (6)—and hence of Eqs. (8) and (9)—implicitly assumes that the energy dependence of the cross section σ is dominated by the Coulomb barrier penetration of the projectile. In other words, the energy dependence of the entrance channel width dominates. Resonant cross sections can be written as a sum of Breit-Wigner terms. It can be shown [5] that for a sufficiently high nuclear level density at the compound nucleus formation energy, the sum of overlapping resonances can be replaced with a sum over averaged widths (or averaged strength functions), leading to the well-established statistical model of compound reactions (Hauser-Feshbach model). Thus, both resonant and Hauser-Feshbach cross sections can be expressed as [5]

$$\sigma \propto \sum_n (2J_n + 1)\frac{X_{\text{in}}^{J_n} X_{\text{fi}}^{J_n}}{X_{\text{tot}}^{J_n}}, \tag{10}$$

with X being either Breit-Wigner widths or averaged Hauser-Feshbach widths, depending on the context. The width of the entrance channel is given by $X_{\text{in}}^{J_n}$; the onewidth of the exit channel, by $X_{\text{fi}}^{J_n}$; and the total width including all possible emission channels, from a given resonance or compound state with spin J_n by $X_{\text{tot}}^{J_n} = X_{\text{in}}^{J_n} + X_{\text{fi}}^{J_n} + \cdots$ Even in the case of the statistical model only few summands in Eq. (10) contribute although the sum runs over all values of J.

It has become common knowledge that a cross section of the form shown in Eq. (10) is determined by the properties of the smaller width in the numerator if no channels other than the entrance and exit channels contribute significantly to $X_{\text{tot}}^{J_n}$. Then $X_{\text{tot}}^{J_n}$ cancels with the larger width in the numerator and the smaller width remains. (The effect is less pronounced and requires more detailed investigation when other channels are nonnegligible in $X_{\text{tot}}^{J_n}$.) In consequence, the energy dependence of the cross section will then be governed by the energy dependence of this smallest X^J. Only if this happens to be a charged-particle (averaged) width in the entrance channel will the use of the standard formula for the Gamow window [Eqs. (8) and (9)] be justified. Because X_{in}^J and X_{fi}^J have different energy dependences, it will depend on the specific energy (weighted by the MB distribution) which of the widths is smaller. A higher plasma temperature will select an energy range at a higher energy. Therefore, the relative sizes of the X^J and thus the energy dependence of the cross sections in the relevant energy range will depend on the plasma temperature. This determines the Gamow windows.

It can be seen immediately that the prerequisite for applying the standard formula may not be met when studying reactions like (p,α) at moderate reaction Q values where one would expect the α width to be smaller than the proton width. Also, for charged-particle capture the standard formula will be problematic as long as the γ width is smaller than the width in the entrance channel. Although astrophysically relevant interaction energies are so small that charged particle widths often become smaller than the radiation widths owing to the Coulomb barrier, reactions in high-temperature environments—such as explosive nucleosynthesis—may still exhibit the opposite relation. Because of the sensitivity of the Gamow window to the relative sizes of the widths and the complicated dependence of the widths on the interaction energy, Gamow windows should be extracted from numerical inspection of the integrand in Eq. (2), and not from the standard formula, which is only applicable for a limited number of cases. This is performed in the following sections.

C. Numerical calculation of Gamow windows

The function

$$\mathcal{F}(E) = \sigma(E) E e^{-E/(kT)} \tag{11}$$

was computed for all targets and reactions given in Ref. [6]. The energies of the maxima $\widetilde{E}_0$ and the widths $\widetilde{\Delta}$ of the peaks of $\mathcal{F}$ were determined for each case. A full table of the results is available as a machine-readable file from EPAPS [7] and on the author's website [8]. With the exception of captures, only reactions with a positive reaction Q value are shown. The effective energy window of the reverse reaction can be found by shifting the energy window by the Q value. For captures reactions with $Q < 0$ are also shown, similar to what is given in Ref. [6], because to minimize stellar plasma effects owing to the thermal population of the target states, it is always preferable to measure captures instead of photodisintegrations [9,10]. Table I is only an abbreviated table to illustrate the kind of information contained in the full table for a few selected examples. The full table contains the Gamow windows of 20 540 charged-particle reactions for temperatures of $0.5 \leqslant T \leqslant 5.0$ GK, involving targets from proton to neutron dripline and with charge numbers of $10 \leqslant Z \leqslant 83$.

It should be noted that the definition of the width $\widetilde{\Delta}$ of the "true" Gamow window used here differs from the definition of the width Δ as used in Eq. (9). The width from the standard approximation is the $1/e$ width of the Gaussian function. However, caution is advised whenever using the energy range defined in such a manner to, for example, derive the energies

TABLE I. Effective energy windows $\widetilde{E}_{\rm hi} - \widetilde{\Delta} \leqslant E \leqslant \widetilde{E}_{\rm hi}$ for a given plasma temperature T. Also listed is the energy $\widetilde{E}_0$ of the maximum in the reaction rate integrand and its shift δ relative to the standard formula. The latter is $\delta = \widetilde{E}_0 - E_0$ relative to the location of the Gamow peak E_0 for charged-particle-induced reactions and $\delta = \widetilde{E}_0 - E_{\rm MB}$ relative to the maximum of the MB distribution at $E_{\rm MB}$ for neutron-induced reactions. This table lists only a few examples. The full table is available from Ref. [7].

Target	Reaction	T (GK)	$\widetilde{E}_{\rm hi}$ (MeV)	$\widetilde{\Delta}$ (MeV)	$\widetilde{E}_0$ (MeV)	δ (MeV)
^{24}Mg	(α,γ)	2.5	2.36	1.05	1.66	−1.16
^{27}Al	(p,γ)	3.5	1.47	1.12	0.65	−0.89
^{40}Ca	(α,γ)	2.0	3.62	1.39	2.85	−0.63
		4.0	4.66	1.97	3.56	−1.97
^{60}Fe	(n,γ)	5.0	1.20	1.20	0.13	−0.30
^{62}Ni	(n,γ)	3.5	1.00	1.00	0.15	−0.15
^{106}Cd	(α,γ)	3.5	10.07	3.44	8.08	−1.17
^{120}Sn	(n,α)	5.0	9.54	4.16	6.92	+6.49
^{144}Sm	(α,γ)	3.5	11.97	3.99	9.90	−1.10
^{169}Tm	(α,γ)	2.0	9.20	2.94	7.61	−0.54
		5.0	13.20	4.27	10.22	−4.79

at which experimental cross sections are to be determined. For the numerically derived true Gamow windows in this work, I found that the area of the peak limited by the $1/e$ width contains only 55%–70% of the total contribution to the integral, which would lead to a similar uncertainty in the reaction rate even when the cross sections within the window were experimentally completely determined. To obtain a better measure for the relevant energy range, for each case (of a given reaction on a specific target at a given temperature) an energy range was numerically determined contributing 90% of the total integral of Eq. (2). This is the width $\widetilde{\Delta}$ quoted in Table I and in the EPAPS table [7].

The energy of the maximum at $\widetilde{E}_0$ determines where the cross sections have the largest weight in the integral. In most cases, however, the relevant energy window is not symmetric around this energy. For a more accurate specification of the energy window, I also give the energy $\widetilde{E}_{\rm hi}$ at the upper end of the window in the tables. Thus, the range of relevant energies is defined as

$$\widetilde{E}_{\rm hi} - \widetilde{\Delta} \leqslant E \leqslant \widetilde{E}_{\rm hi}. \tag{12}$$

In the following I present general observations and discuss selected cases of interest. For comparison to the standard approximation formula, I define a shift $\delta = \widetilde{E}_0 - E_0$ relative to the location of the Gamow peak energy E_0 as given by the standard approach. In general, at higher temperatures and for increasing charge numbers, the shifts $|\delta|$ will be larger. These main effects are moderated, however, by the involved interplay of different Coulomb barriers in different channels and different reaction Q values, leading to a more complicated energy dependence of the widths and thus also of the cross sections.

Because neutrons do not experience a Coulomb barrier and neutron widths are larger than charged particle widths at low

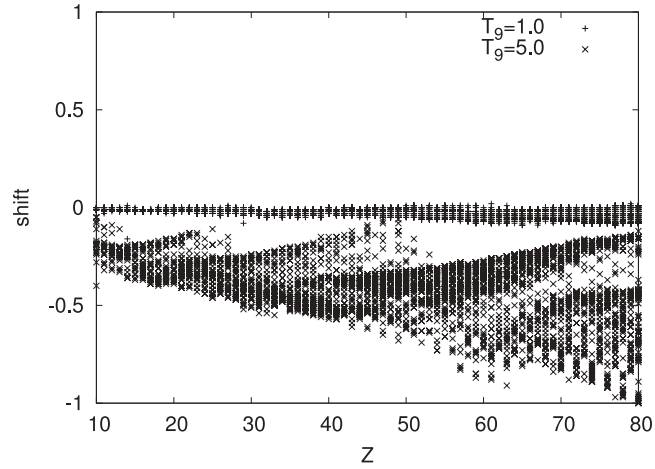

FIG. 1. Shifts δ (MeV) of the maximum of the integrand relative to E_0 of the Gaussian approximation as a function of the target charge Z for (p,n) reactions at two temperatures. Almost no shift is observed at $T_9 = 1.0$ and shifts remain small for $T_9 = 5.0$.

energies in most cases, the charge and temperature effects can be most clearly seen in (p,n) and (α, n) reactions (Figs. 1 and 2). In both types of reactions there are no or only small shifts at $T_9 = 1.0$ but large shifts at $T_9 = 5.0$. The magnitude of the shifts is generally larger for the (α, n) reactions (note the different scale of the figures) owing to the higher charge of the α particle. The $|\delta|$ also increase with increasing target charge Z in both cases. The shifts are always to a lower energy because the energy dependence of the neutron widths selects an effective energy close to $E_{\rm MB}$ (see Sec. III) which is always below E_0.

Charged-particle capture is important in a variety of astrophysical processes. As mentioned in Sec. II B, for capture reactions the applicability of the standard approximation depends on the size of the γ width X^J_γ relative to the projectile width $X^J_{\rm in}$. When $X^J_\gamma \ll X^J_{\rm in}$, one would assume that there is

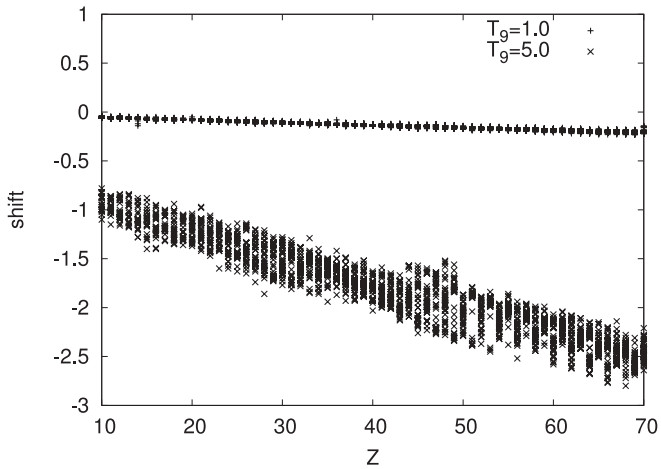

FIG. 2. Shifts δ (MeV) of the maximum of the integrand relative to E_0 of the Gaussian approximation as a function of the target charge Z for (α, n) reactions at two temperatures. Almost no shift is observed at $T_9 = 1.0$ and shifts reach a few mega–electron volts for $T_9 = 5.0$.

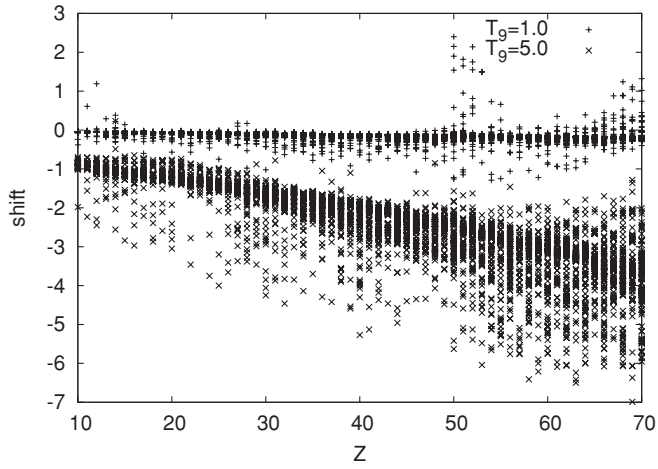

FIG. 3. Shifts δ (MeV) of the maximum of the integrand relative to E_0 of the Gaussian approximation as a function of the target charge Z for (α,γ) reactions at two temperatures. Almost no shift is observed at $T_9 = 1.0$ but shifts become large at $T_9 = 5.0$.

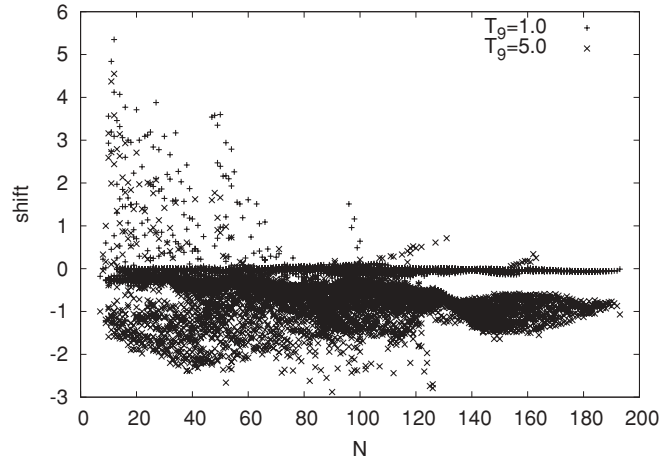

FIG. 4. Shifts δ (MeV) of the maximum of the integrand relative to E_0 of the Gaussian approximation as a function of the target neutron number N for (p,γ) reactions at two temperatures. Almost no shift is observed at $T_9 = 1.0$, except for proton-rich nuclei with a negative reaction Q value. Shifts remain smaller than for (α,γ) at $T_9 = 5.0$.

no Gamow window, as the energy dependence of the γ width does not show as strong an increase with increasing energy as a charged-particle width [1]. However, effectively the Gamow window is shifted only to a much lower energy. This can be understood by the fact that the integration limit in Eq. (2) starts at zero energy and thus will always include either a region where $X^J_{\rm in} \ll X^J_\gamma$ and the Coulomb penetration is competing with the decay of the MB distribution at larger energies or the low-energy region of the MB distribution suppressing a weakly energy-dependent radiation width. Both cases lead to a peak in the integrand $\mathcal{F}$, although the "peak" may be located so that it closely approaches zero energy. Figure 3 shows a similar temperature dependence of the shifts for α captures as for (α, n), although the magnitude of the shifts is larger. These shifts are caused by the fact that at a higher T energy, regions with $X^J_\alpha \gg X^J_\gamma$ receive a larger weight by the MB distribution. Positive shifts appear for cases with $Q < 0$, simply because the Gamow energy E_0 derived from Eq. (8) is below the (α,γ) threshold and the actual energy window opens at higher energy. The situation is similar for (p,γ) reactions but the temperature dependence is not as pronounced. The positive shifts occur for proton-rich targets at the proton dripline, as shown in Fig. 4, plotting the shifts versus the neutron number N.

The astrophysical importance of capture reactions warrants study for a few cases in more detail. As already pointed out [1,3], it was experimentally found that resonances below the Gamow window, as defined by the standard approximation formulas, significantly contribute to the reaction rate for certain capture reactions, for example, ^{24}Mg$(\alpha,\gamma)^{28}$Si and ^{27}Al$(p,\gamma)^{28}$Si. The results for these reactions are reported in Table I. Figure 5 shows a comparison of the actual integrands $\mathcal{F}$ and the Gaussian functions obtained by application of Eqs. (8) and (9). This can be directly compared to Fig. 3.24 of Ref. [1], where the relative contributions of resonances are compared to the Gamow window derived from the standard approximation (for a brief discussion of the relevance of the Gamow window for narrow resonances, see Sec. IV). The present results show that the approximation is not valid and the actual Gamow window is shifted to a lower energy, in agreement with what was found in Ref. [1] but quantifying the relevant energy window. A similar case is ^{40}Ca$(\alpha,\gamma)^{44}$Ti, where the effective energy window is also considerably shifted to a lower energy. A plot comparing the actual integrand of the reaction rate with the Gaussian approximation is given in Ref. [11]. A further example is the reaction ^{169}Tm$(\alpha,\gamma)^{173}$Lu, shown in Fig. 6. Again, the shift is considerable at a temperature reached in explosive nucleosynthesis. It is larger than the shifts for lighter targets because of the larger Coulomb barrier. The increasing asymmetry of the peak with increasing temperature can also clearly be seen.

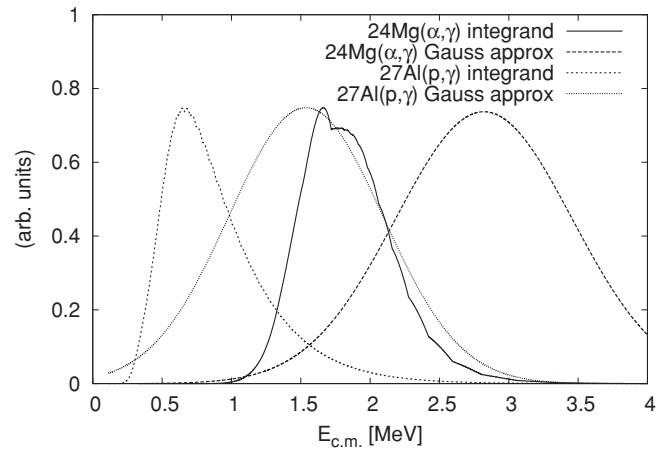

FIG. 5. Comparison of actual reaction rate integrand $\mathcal{F}$ and Gaussian approximation of the Gamow window for the reactions ^{24}Mg$(\alpha,\gamma)^{28}$Si at $T = 2.5$ GK and ^{27}Al$(p,\gamma)^{28}$Si at $T = 3.5$ GK. The integrands and Gaussians have been arbitrarily scaled to yield similar maximal values.

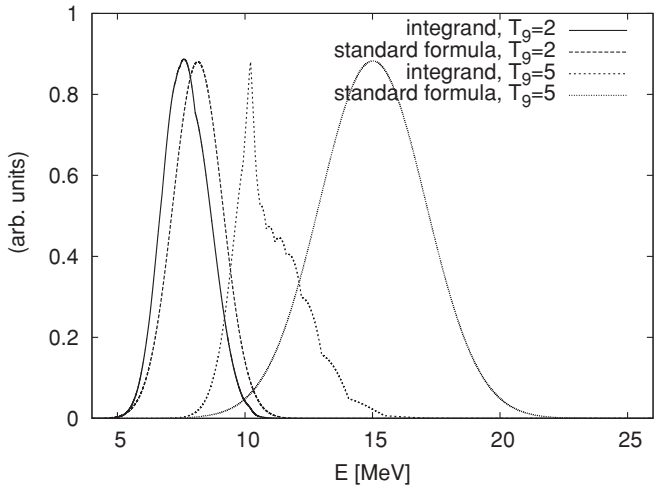

FIG. 6. Comparison of actual reaction rate integrands $\mathcal{F}$ and Gaussian approximations of the Gamow window for the reaction ^{169}Tm$(\alpha,\gamma)^{173}$Lu at $T = 2$ and 5 GK. The integrands and Gaussians have been arbitrarily scaled to yield similar maximal values. While the shift is small for $T_9 = 2$, it is about 5 MeV at $T_9 = 5$. Also, the asymmetry of the integrand can be clearly seen at $T_9 = 5$.

Finally, we might expect that reactions with charged particles in both channels show the most complicated dependence on temperature and charge. However, it is found that the obtained shifts are negligible at low temperatures, which can be explained by the fact that the energy dependence of the entrance width dominates at low interaction energies. Figure 7 shows that at $T_9 = 5$, similar values of the shifts are obtained in (α, p) reactions as in (α,n) reactions, smaller than for (α,γ). The shifts are also negligible at low temperatures for (p,α) reactions but larger and *positive* ($\delta > 0$) shifts are found at high temperatures (see Fig. 8). This is because the proton widths quickly become larger than the α widths at

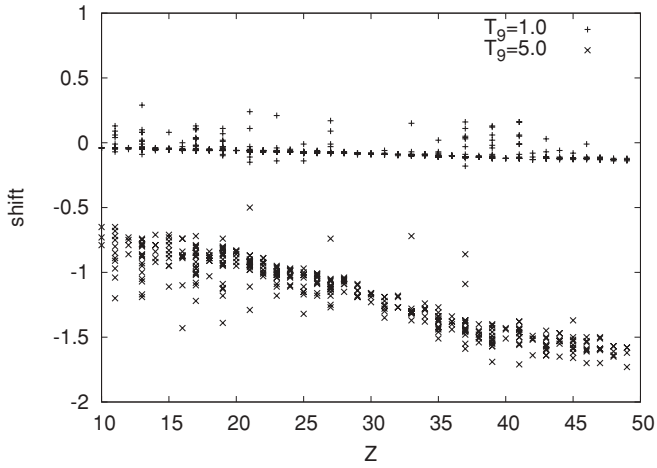

FIG. 7. Shifts δ (MeV) of the maximum of the integrand relative to E_0 of the Gaussian approximation as a function of the target charge Z for (α, p) reactions at two temperatures. Almost no shift is observed at $T_9 = 1.0$ and shifts reach a few mega–electron volts for $T_9 = 5.0$.

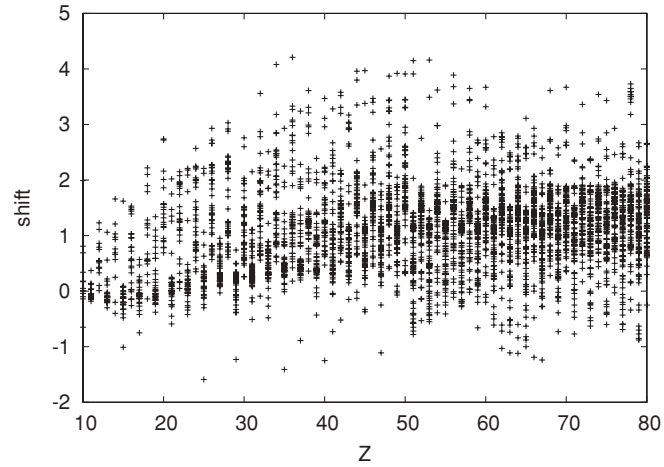

FIG. 8. Shifts δ (MeV) of the maximum of the integrand relative to E_0 of the Gaussian approximation as a function of the target charge Z for (p,α) reactions at $T = 5$ GK. The shifts are larger as for (α, p) reactions and they are positive.

higher energies and this leads to a dominance of the α-width energy dependence. Owing to the higher Coulomb barrier, the effective energy window is then found at a higher energy compared to the Gamow window calculated for protons. This effect is shown in more detail in Fig. 9 for ^{112}Sn$(p,\alpha)^{109}$In at $T_9 = 5.0$.

III. REACTIONS WITH NEUTRONS

Neutrons are not subject to a Coulomb barrier and therefore a Gamow peak cannot be defined as in Eq. (3). Nevertheless, an effective energy range can be found because $\sigma(E)$ usually is a slowly varying function that can be parameterized depending

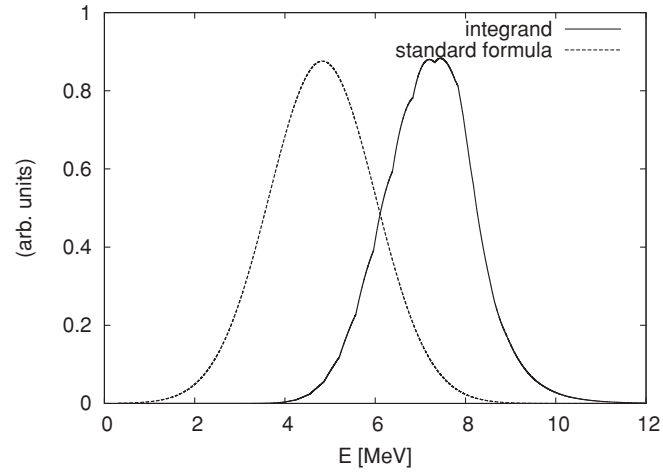

FIG. 9. Comparison of the actual reaction rate integrand $\mathcal{F}$ and the Gaussian approximation of the Gamow window for the reaction ^{112}Sn$(p,\alpha)^{109}$In at $T = 5$ GK. The two curves have been arbitrarily scaled to yield similar maximal values. The maximum of the integrand is shifted by several mega–electron volts to energies higher than the maximum E_0 of the Gaussian.

on the dominant partial wave, that is, $\sigma \propto 1/\sqrt{E}$ for s waves, $\sigma \propto \sqrt{E}$ for p waves, and $\sigma \propto E^{3/2}$ for d waves. Then the integrand $\mathcal{F}$ defined in Eq. (2) will exhibit a peak mainly determined by the peak of the MB distribution $E_{\rm MB} = kT$, only slightly shifted for partial waves $\ell > 0$, owing to the angular momentum barrier. An often used approximation is [4,12]

$$E_{\rm eff} \approx 0.172 T_9 \left(\ell + \frac{1}{2}\right), \tag{13}$$

$$\Delta_{\rm eff} \approx 0.194 T_9 \sqrt{\ell + \frac{1}{2}}, \tag{14}$$

giving the effective energy window $E_{\rm eff} \pm \Delta_{\rm eff}/2$ MeV for neutrons with energies less than the centrifugal barrier. This expression is not as handy as the one for the charged-particle Gamow peak because the dominant partial wave is not known a priori. Nevertheless, the shifts with partial wave are comparatively small and the assumption of s waves is sufficient to define a useful energy window.

A straightforward application of Eqs. (13) and (14) will not be valid in all cases. Just as was the case with the approximation for charged projectiles in Sec. II, the derivation of the formula implicitly assumes that the energy dependence of the cross section is determined by the neutron projectile. This is justified for low-energy direct capture or reactions through wings of broad resonances. In the general resonant case (and the case of averaging over a large number of resonances as performed in statistical model calculations), however, the energy dependence of the exit channel width can become important and strongly modify the effective energy window.

Similar to the reactions with charged projectiles discussed in Sec. II, the actual effective energy windows were derived by calculating $\mathcal{F}(E)$ from Eq. (11) and numerically determining its maximum and the range of the main contributions to the rate integral (Eq. (2)). Neutron capture as well as (n,p) and (n,α) reactions are also included in the EPAPS table [7]. Just as for charged-particle reactions only reactions with positive Q values are listed, except for (n,γ) reactions, which also include a number of endothermic neutron captures at the dripline. This amounts to a total of 8862 neutron-induced reactions. Table I lists a few selected examples. The shifts δ given for neutron-induced reactions are relative to the peak of the MB distribution, as this defines the location of the peak for neutron s waves: $\delta = \widetilde{E}_0 - E_{\rm MB}$. The effective energy window is again given by Eq. (12).

The shifts are zero or small for most neutron captures, except for those close to the neutron dripline. One would assume that this confirms the validity of Eqs. (13) and (14) for (n,γ) reactions. However, it is rather because the total γ widths, being smaller than the neutron widths in Eq. (10), have a comparatively weak energy dependence and do not move the maximum of the integrand $\mathcal{F}$ from the one given by the MB distribution. This explains why all of the maxima $\widetilde{E}_0$ are more or less identical to $E_{\rm MB}$ and thus also $\widetilde{E}_0 \approx E_{\rm eff}$, with the $E_{\rm eff}$ for $\ell = 0$. A different behavior is found only at low neutron separation energies, where either γ widths show a stronger energy dependence or neutron widths become the smallest

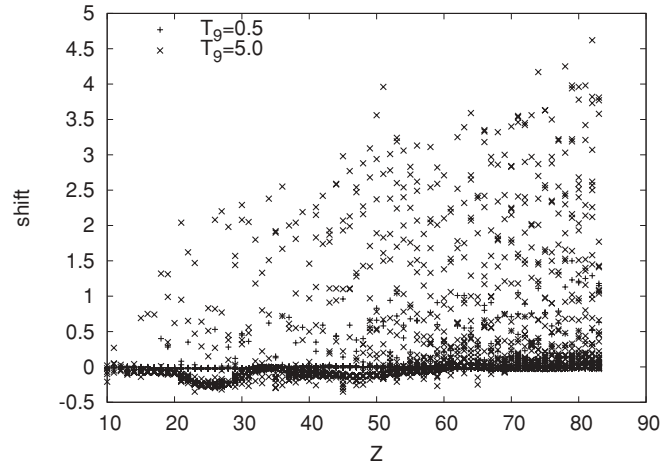

FIG. 10. Shifts δ (MeV) of the maximum of the integrand relative to $E_{\rm MB}$ as a function of the target charge Z for (n,p) reactions at two temperatures. Almost no shift is observed at $T_9 = 0.5$ but shifts become large at $T_9 = 5.0$.

widths in the reaction channels. Only in the latter case will different neutron partial waves be important in Eq. (13).

Despite the small absolute shifts for neutron captures, it becomes apparent that the relevant energy window as defined by Eq. (12) reaches down to the reaction threshold if one desires to determine the reaction rate with a high integration accuracy, even at high plasma temperatures (see also the examples in Table I).

Larger shifts are found for reactions with charged particles in the exit channel. Contrary to most cases discussed in Sec. II, the shifts are positive for the majority of neutron-induced reactions because the Coulomb barrier penetration in the exit channel moves the energy window to a higher energy. As expected, the shifts are larger for increased temperature, increased charge of the compound nucleus, and increased charge of the ejectile. Figures 10 and 11 illustrate these dependences for (n,p) and (n,α) reactions. For $T_9 = 0.5$

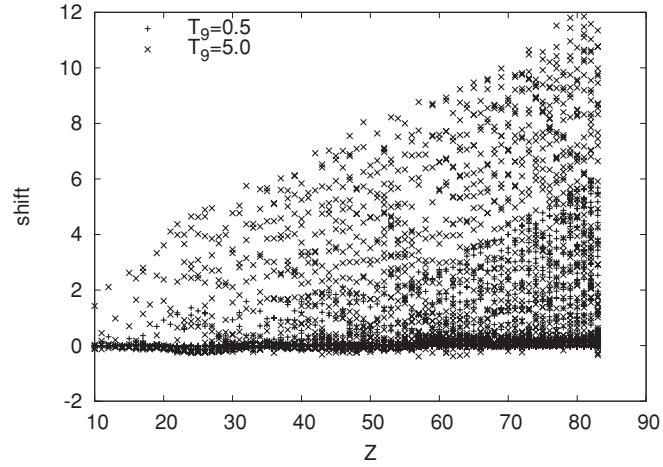

FIG. 11. Shifts δ (MeV) of the maximum of the integrand relative to $E_{\rm MB}$ as a function of the target charge Z for (n,p) reactions at two temperatures. Almost no shift is observed at $T_9 = 0.5$ but shifts become very large at $T_9 = 5.0$.

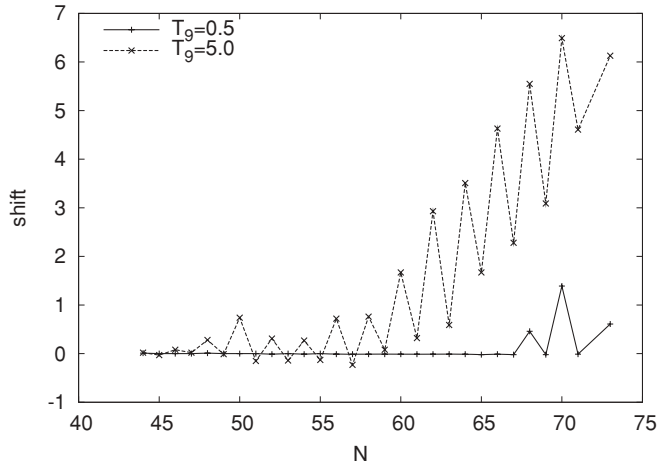

FIG. 12. Shifts δ (MeV) of the maximum of the integrand relative to E_{MB} as a function of the target neutron number N for (n,α) reactions on Sn isotopes at two temperatures. Almost no shift is observed at $T_9 = 0.5$ but shifts become large at $T_9 = 5.0$ for the neutron-rich isotopes with a small reaction Q value.

the shifts are close to zero, whereas they can reach several mega–electron volts at $T_9 = 5$. The behavior within an isotopic chain is shown in Fig. 12 for (n,α) on Sn isotopes. Again, for low temperatures the effective energy window is barely shifted from the one predicted by the standard formula. With increasing temperature the shift becomes larger. The shifts for neutron-rich nuclei are larger, as the energy dependence of the α width becomes stronger with decreasing Q value.

IV. CONCLUDING DISCUSSION

It must be pointed out that the preceding discussion has made implicit assumptions that have to be scrutinized in any application of the results. An obvious assumption is that the cross sections used are correct. The results shown here were obtained with the FRDM set given in Ref. [6]. Although transmission coefficients (and thus widths) are affected by low-lying nuclear states that can be populated in a reaction, the derived energy *windows* should be robust because the gross energy dependence of the cross section is the relevant quantity and not its absolute value. At astrophysical temperatures the MB distribution always favors energies below the Coulomb barrier. Therefore, the energy dependence of charged-particle widths is dominated by the Coulomb barrier penetration. Because the energy dependences of widths in all channels may contribute, the energy windows are also sensitive to the reaction Q values. Accordingly, updates to masses may affect the conclusions close to the driplines. This also holds for neutron capture reactions. Although the selection of contributing partial waves strongly depends on the spectroscopy of a nucleus, the shape of the MB distribution is not strongly modified when folded with the energy dependence of any relevant partial wave, as explained in Sec. III. Therefore the relevant energy window for neutron capture is defined by the peak of the MB distribution.

Another source of concern may be the use of statistical model Hauser-Feshbach cross sections for nuclei with a low level-density close to the driplines, especially for rates at low plasma temperatures. As explained previously, the energy windows are mostly determined by the Coulomb barrier penetration in the different channels or by the MB distribution. This will also hold for direct reactions. As explained here, the derived effective energy windows remain valid even when narrow resonances contribute, and therefore this is not a limitation of the method.

The final assumption seems to be that the cross sections are smooth without isolated resonance features. The notion of a single Gamow peak loses its validity when narrow, isolated resonances dominate the reaction rate. In this case, the Gamow window would be fragmented into several Gamow peaks of different importance, depending on the resonance strengths. It can be shown, nevertheless, that the notion of an effective energy window remains valid and that only resonances within the energy window contribute significantly to the reaction rate (for details see, e.g., Ref. [1]). This applies provided that the energy windows are derived as demonstrated here. It does not make a statement about the relative importance of resonances because this depends on the actual resonance strengths, not just on the energy dependence of the widths.

To summarize, a complete numerical study of the effective energy windows for nuclear reaction rates has been performed for reactions induced by nucleons and α particles. It has been shown that the actual energy range of relevant cross sections differs considerably from the ranges obtained by application of the standard formulas. The origin of this difference has been explained, and extensive tables of the actual energy windows given. This will be important for further theoretical improvements of reaction rates as well as for helping to design experiments to measure cross sections at energies of astrophysical importance.

ACKNOWLEDGMENTS

Discussions with R. D. Hoffman are acknowledged. This work was supported by Swiss NSF Grant No. 200020-122287.

[1] C. Iliadis, *Nuclear Physics of Stars* (Wiley VCH, Berlin, 2007).
[2] C. S. Rolfs and W. S. Rodney, *Cauldrons in the Cosmos* (University of Chicago Press, Chicago, 1986).
[3] J. R. Newton, C. Iliadis, A. E. Champagne, A. Coc, Y. Parpottas, and C. Ugalde, Phys. Rev. C **75**, 045801 (2007).
[4] T. Rauscher, F.-K. Thielemann, and K.-L. Kratz, Phys. Rev. C **56**, 1613 (1997).

[5] P. Descouvemont and T. Rauscher, Nucl. Phys. A **777**, 137 (2006).
[6] T. Rauscher and F.-K. Thielemann, At. Data Nucl. Data Tables **79**, 47 (2001).
[7] See supplementary material at http://link.aps.org/supplemental/10.1103/PhysRevC.81.045807 for a ASCII file containing the full table of energy windows and shifts.
[8] http://nucastro.org/tables.html.
[9] G. G. Kiss, T. Rauscher, Gy. Gyürky, A. Simon, Zs. Fülöp, and E. Somorjai, Phys. Rev. Lett. **101**, 191101 (2008).
[10] T. Rauscher, G. G. Kiss, Gy. Gyürky, A. Simon, Zs. Fülöp, and E. Somorjai, Phys. Rev. C **80**, 035801 (2009).
[11] R. D. Hoffman *et al.*, Astrophys. J. (in press); arXiv:1003.0110.
[12] R. V. Wagoner, Astrophys. J. Suppl. **18**, 247 (1969).